Photon-ALP oscillations with ELMAG

M. Kachelrieß[a,*] **and J. Tjemsland**[a,*]

[a]*Institutt for fysikk, NTNU, Trondheim, Norway*

E-mail: jonas.tjemsland@ntnu.no

ELMAG is a Monte Carlo program made to simulate electromagnetic cascades initiated by high-energy photons interacting with the extragalactic background light. Photons propagating in an external magnetic field may oscillate into axions or axion-like particles (ALPs). Such oscillations lead to characteristic features in the energy spectrum of high-energy photons from astrophysical sources that can be used to probe the existence of ALPs. We have implemented ALPs into ELMAG, complementing thereby existing descriptions of photon-ALP oscillations with a Monte Carlo treatment of high-energy photon propagation and interactions. Here, we discuss the implementation of ALPs into ELMAG, review the expected signatures of photon-ALP oscillations and stress the importance of a proper treatment of magnetic fields. Furthermore, we introduce a new statistical test using the discrete power spectrum, which may significantly improve the sensitivity of astrophysical ALP searches.

---

*Speaker

1. Introduction

In 1977, Peccei and Quinn postulated the existence of an additional spontanously broken U(1) symmetry as a solution to the strong CP problem [1, 2]. Since a two-gluon-vertex is needed to solve the strong CP problem, the Nambu-Goldstone boson associated with the broken symmetry will acquire a small mass from pion mixing [3, 4]. In addition, it will inherit a characteristic two-photon vertex from the pion, $\mathcal{L} = -g_{a\gamma}F_{\mu\nu}\tilde{F}^{\mu\nu} = g_{a\gamma}\vec{E} \cdot \vec{B}$. Despite its small mass, the axion turns out to be a suitable cold dark matter candidate if it is produced in e.g. the misalignment mechanism [5–8]. In this scenario, the axionic dark matter is produced by coherent oscillation of the axion field due to an initial misalignment of the parameter ϑ around the QCD phase transition.

In order to be more general, it is common to work with a general class of pseudo-scalar bosons with the same characteristic two-photon coupling as the axion. Such particles are known as axion-like particles (ALPs), and although they do not solve the strong CP problem, they are theoretically well motivated as they are naturally present in a number of Standard Model extensions, including string theories [9, 10]. The ALPs are thus characterised by two parameters: their mass m_a and their photon coupling $g_{a\gamma}$. Photons propagating through an external magnetic field may convert into ALPs[1], and vice versa, due to the two-photon–ALP vertex. This leads to the phenomenon known as *photon-ALP oscillation*.

The leading limits $g_{a\gamma} \lesssim 10^{-20}$ eV for $m_a \lesssim 10^{-6}$ eV are set by the non-detection of photon-ALP oscillations in astrophysical observations [11–14] and the non-detection of spectral features expected from the Primakoff effect [15–18]. Searches based on photon-ALP oscillations depend, however, strongly on the treatment of the magnetic fields. Astrophysical observations do not yet constrain any part of the parameter space where the ALP is a viable dark matter candidate [19]. However, one expects a significant improvement with the upcoming Cherenkov Telescope Array (CTA) [20].

In this work, we review the implementation of ALPs into ELMAG and discuss the signatures expected from photon-ALP oscillations in photon spectra from gamma ray sources. This work complements existing codes (e.g. gammaALPs [21] and ALPro [22]) by considering a Monte Carlo description of the photon propagation and interactions. Furthermore, we discuss the importance of a proper treatment of the magnetic field environments. Finally, we introduce a promising statistical method for astrophysical searches for photon-ALP oscillations. Most of the discussions are based on Ref. [23].
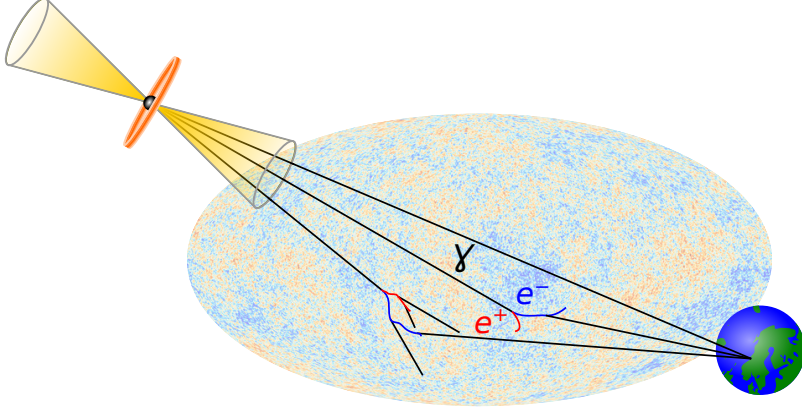
2. ELMAG

ELMAG[2] is a Monte Carlo program written in Fortran 90 made to simulate electromagnetic cascades initiated by high-energy photons[3] interacting with the extragalactic background light (EBL) [24, 25]. The photons must be above the pair production threshold to initiate a cascade, meaning $E \gtrsim 10^{10}$ eV on interactions with the EBL [26]. The general idea is visualised in Fig. 1:

---

[1]We will from now on refer to axions and ALPs collectively as 'ALPs'.

[2]The code is freely available at http://elmag.sourceforge.net.

[3]We are mainly interested in primary photons with energies above the pair production threshold and secondary photons with energies $\gtrsim$ MeV.

Figure 1: Overview of the process of electromagnetic cascades simulated by ELMAG as explained in the text (CMB map © ESA and the Planck Collaboration).

high energy gamma-rays will produce an electron-positron pair upon interaction with photons from the EBL, $\gamma + \gamma_{\text{EBL}} \rightarrow e^+ e^-$. The electrons and positrons will be deflected by the magnetic fields before they in turn may upscatter EBL photons, $e^{\pm} + \gamma_{\text{EBL}} \rightarrow e^{\pm} + \gamma$. This implies that photons produced in the cascade might have a slightly changed arrival direction, thus producing a gamma-ray halo around the source, as well as a time delay. The main effect is in any case a strong attenuation of the photon flux at energies $E \gtrsim 10^{12}$ eV. The mean free path length at 10 TeV is of order 10 Mpc for photons and 10 kpc for the electrons. Most of the propagation is therefore in the form of a photon which travels in a straight line.

Given the source properties (source spectrum, orientation of a jetted source and distance), ELMAG computes the resulting energy spectrum on Earth, the observation angle and the time delay. The computations can be done either in 1D in the small angle approximation, or in 3D using a Lorentz force solver. Currently, the program includes e.g. adiabatic energy losses, synchrotron losses, plasma instabilities and detector angular resolution. Furthermore, several common models for the EBL and plasma instabilities are implemented. The magnetic field is either supplied to the program as tabulated data, or described as a Gaussian turbulent field (normalised such that the energy density stored in the field is given by $B_{\text{rms}}^2/2$).

3. Photon-ALP oscillations with ELMAG

If ALPs exist, photons propagating in an external magnetic field may interact with a virtual photon from the magnetic field and thereby transform into an ALP via the two-photon–ALP coupling. This effect leads to so-called photon-ALP oscillation which can be described physically as an oscillation between two mass eigenstates with different masses, similar to neutrino oscillations. That is, the conversion probability of a photon into an ALP can be written as

$$P_{\gamma \rightarrow a} = |\langle a | \psi(t) \rangle|^2 = \sin^2(2\theta) \sin\left(\frac{z}{2E}[m_1^2 - m_2^2]\right), \tag{1}$$

where m_1 and m_2 are the masses of the two mass eigenstates, E is the energy and z is the distance travelled. Since the effective mass of the photon depends on its refractive index, n, the oscillation

length will depend on the propagation environment and energy in addition to the ALP mass. For concreteness, we will denote the superposition of a photon and an ALP as a *phaxion*.

More precisely, the propagation of a high energy phaxion in the z-direction can be described by the linearised equation of motion [27]

$$(E + \mathcal{M} - \mathrm{i}\partial_z)\phi(z) = 0, \tag{2}$$

where

$$\mathcal{M} = \begin{pmatrix} (n_\perp - 1)E & 0 & 0 \\ 0 & (n_\parallel - 1)E & g_{a\gamma}B_\perp/2 \\ 0 & g_{a\gamma}B_\perp/2 & -2m_a/E \end{pmatrix} \tag{3}$$

is the mixing matrix and $\phi(z) = (A_\perp \ A_\parallel \ a)^{\mathrm{T}}$ is the phaxion wave function. Here, $\perp$ ($\parallel$) denotes the direction perpendicular (parallel) to the transverse magnetic field $\vec{B}_\perp \equiv \vec{B}_x + \vec{B}_y$. Note that only the photon polarisation state parallel to $\vec{B}_{\mathrm{T}}$ will mix with the ALP, which can be understood by the fact that the angular momentum needed to transform the spin-1 photon to the spin-0 ALP has to be supplied by the magnetic field.
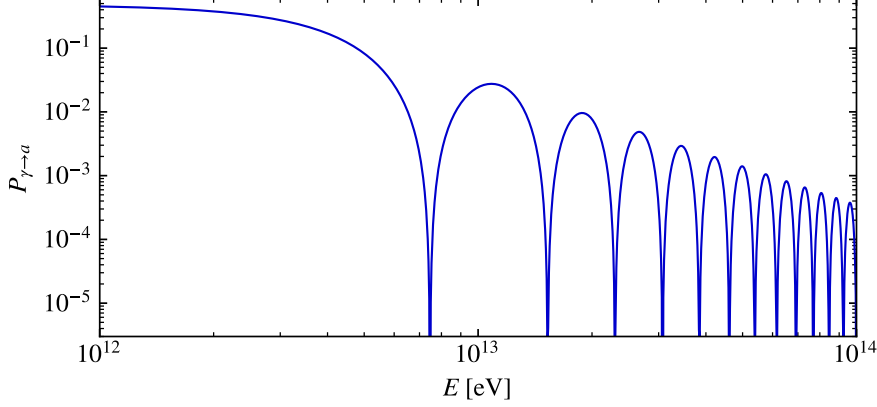
The inclusion of ALPs into ELMAG has several advantages compared to existing (semi-) analytical approaches to photon-ALP oscillations (see e.g. Ref. [28] and references therein): first, the method can treat any magnetic field configuration. Second, additional effects like varying electron density and EBL density can be included. Third, the absorbtion of photons is by default taken into account on an event-by-event basis, and cascade photons are therefore included in the analysis. This allows us to take into account ALPs in other studies on electromagnetic cascades. Finally, polarisation effects are considered by default. The latter two are also improvements compared to existing codes (e.g. Ref. [21]) at the expense of being more computationally demanding. The implementation of ALPs into ELMAG follows the following algorithm:

1. Consider a pure photon with an energy drawn according to the chosen source spectrum.

2. Draw the interaction length, λ, of a photon at the current position, s.

3. Propagate the phaxion, $\phi(z)$, from s to $s + \lambda$ according to the phaxion equation of motion.

4. If $|\langle a|\phi(s + \lambda)\rangle|^2 < r$ for a randomly chosen number $r \in [0, 1]$, the phaxion collapses into a photon and undergoes pair production at position $s + \lambda$. If not, go to 2 with $s \to s + \lambda$.

5. Treat the electromagnetic cascade that arises, and for each photon go to 2.

It is common to consider an unpolarised gamma ray beam, which in our Monte Carlo can be achieved by choosing a random linear polarisation in step 1. Step 1, 2 and 5 are already implemented in ELMAG.

For concreteness, we will here focus on extragalactic magnetic fields, photons above TeV energies, small ALP masses ($m_a \lesssim 10^{-10}$) and fix $g_{a\gamma} = 10^{-20}$ eV. As we will see, this range of parameters is relevant for the upcoming Cherenkov telescope array (CTA). A complete discussion for a general magnetic field strength, energy and ALP mass is given in Ref. [23]. To get a feeling for the effect of photon-ALP oscillations, we plot if Fig. 2 the analytical solution for a phaxion travelling through homogeneous magnetic field with strength $B_{\mathrm{T}} = 5$ nG. From the figure, one

can clearly see the transition from the strong mixing regime, where the off-diagonal elements of the mixing matrix dominates, to the regime where the CMB dominates the refractive index. A similar transition whose location depends on the ALP mass takes place at lower energies. The same characteristics are present even in turbulent magnetic fields (see e.g. Fig. 4 in Ref. [23]).
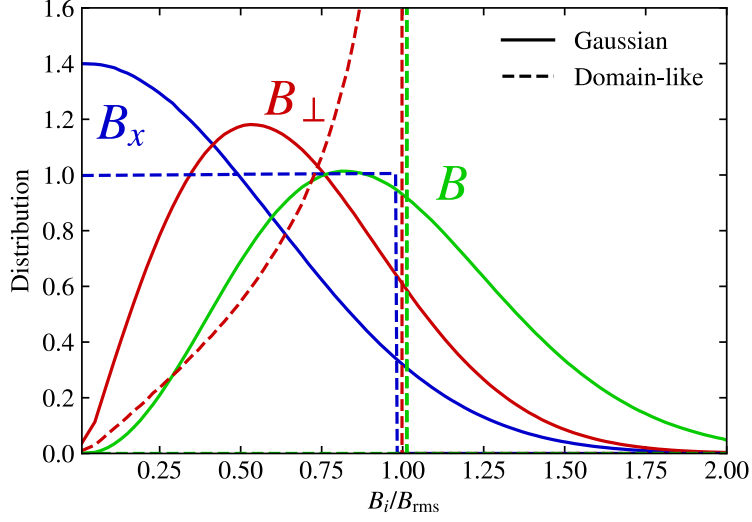

Figure 2: The photon conversion propability for a photon propagating a distance 10 Mpc through a homogeneous magnetic field with strength 5 nG is plotted as a function of photon energy.

4. Comment on the treatment of the magnetic fields

In this section, we will comment on the importance of a proper treatment of the magnetic field distribution in studies of photon-ALP oscillations (see also Refs. [28–30] for different discussions on the same topic). For concreteness, we will consider as examples Gaussian turbulent fields and so-called domain-like turbulence. In the latter case, the magnetic field along the line of sight is divided into patches of size L_{coh} with homogeneous magnetic fields. The field strength in each patch is fixed at B_{tot} (which here is set equal to B_{rms}), while the direction of each patch is chosen randomly. Even if the field is unphysical, it is commonly used in the litterature, see Refs. [13, 14, 21, 28, 29, 31–36] for some recent examples. This approach is certainly invalid when $L_{osc} \ll L_{coh}$ since the magnetic field in this case is essentially probed by one or more complete oscillations for each coherence length, meaning that the photon-ALP oscillations depend on the field fluctuations at scales smaller than the coherence length. Even when $L_{osc} \gg L_{coh}$, the "cosmic variance" in the magnetic field distribution may have a considerable effect on the oscillations. To visualise this, we plot in Fig. 3 the distributions of the magnetic fields for a Gaussian (solid lines) and domain-like (dashed lines). It is clear that the variance in B_T, and thus the mixing term $g_{a\gamma}B_\perp/2$, is much larger for the Gaussian turbulence than the domain-like turbulence.

The cosmic variance implies that the onset of the ALP wiggles has a larger variance and thus the wiggles in the survival probability are smoothed out. Furthermore, the simple domain-like turbulence has on average shorter convergence time. As we will see in the next section, the former implies that irregularities in photon spectra are more pronounced and the latter that the transparency of the Universe may be overestimated with the domain-like turbulence.

Figure 3: The distribution of the magnetic field strength for Gaussian turbulent fields (solid lines) and the domain-like field (dashed lines) is compared. The field strength in x-direction is shown in blue, in the transverse direction in red and total strength in green.

5. Signatures of photon-ALP oscillations on high energy photon spectra

There are two signals that are typically considered in the search for astrophysical photon-ALP oscillations: an increased opacity of the Universe and "irregularities" in photon spectra. The main focus is here on the "irregularities". As we will see, these irregularities follow a clear pattern that can be exploited to increase the sensitivity of ALP searches, and we will therefore refer to them as *ALP wiggles*.
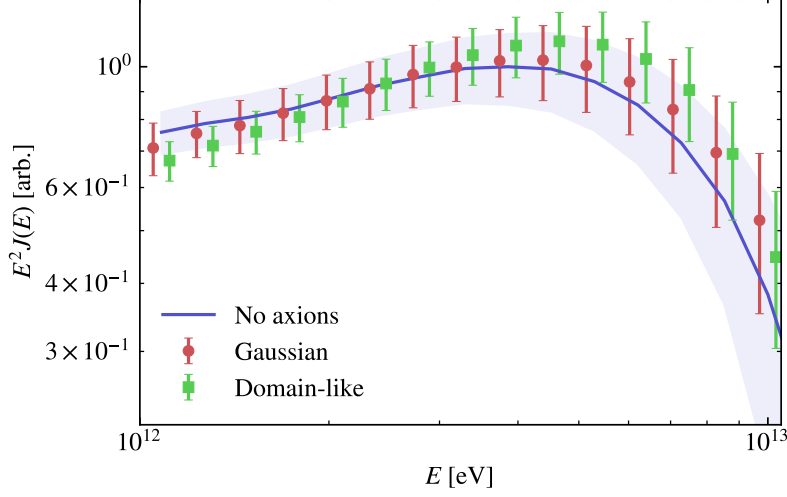
For concreteness, we will consider a source at redshift $z = 0.1$ with a power-law spectrum $dN/dE \propto E^{-1.2}$. We consider a turbulent extragalactic magnetic field with $B_{rms} = 5$ nG and $L_c = 1$ Mpc. For the Gaussian turbulent field, a Kolmogorov spectrum divided into 100 modes between $L_{max} = 5$ Mpc and $L_{min} = 0.01$ Mpc is used. We inject photons at energies between 1 TeV and 100 TeV and stop the simulations when 1000 photons in the same energy range reaches $z = 0$. We simulate 1000 realisations of the magnetic field in all cases. In order to account for detector energy resolution, we scramble the final energy according to the CTA energy resolution [37].

5.1 Increased opacity of the Universe

Photon-ALP oscillations will effectively increase the mean free path length in the EBL since ALPs travel practically without any interactions [38], and has the potential to explain the observed optical depth of TeV photons in the Universe [39]. Perhaps more importantly, the increased opacity can be used as a probe for photon-ALP oscillations [29].

The effect of the increased opacity can be seen in Fig. 4, in which we have plotted the photon spectrum obtained after averaging over the realisations of the magnetic fields. The error bars corresponds to the 1σ statistical variation in the resulting photon spectra. At $E \gtrsim 10^{13}$ eV, the flux obtained with ALPs tend to be larger than without, which leads to an increased opacity of the

Universe[4]. Interestingely, the spectra using the domain-like and Gaussian turbulent fields are, on average, significantly different. This difference becomes even more clear at larger redshifts [23, 29].

Figure 4: Average photon spectrum at Earth obtained using 1000 realisations for a Gaussian turbulent field (red circles) and a domain-like field (green squares). The errorbars indicate the 1σ statistical variation in the realisations of the magnetic fields. The spectrum without ALPs is shown in blue for comparison.
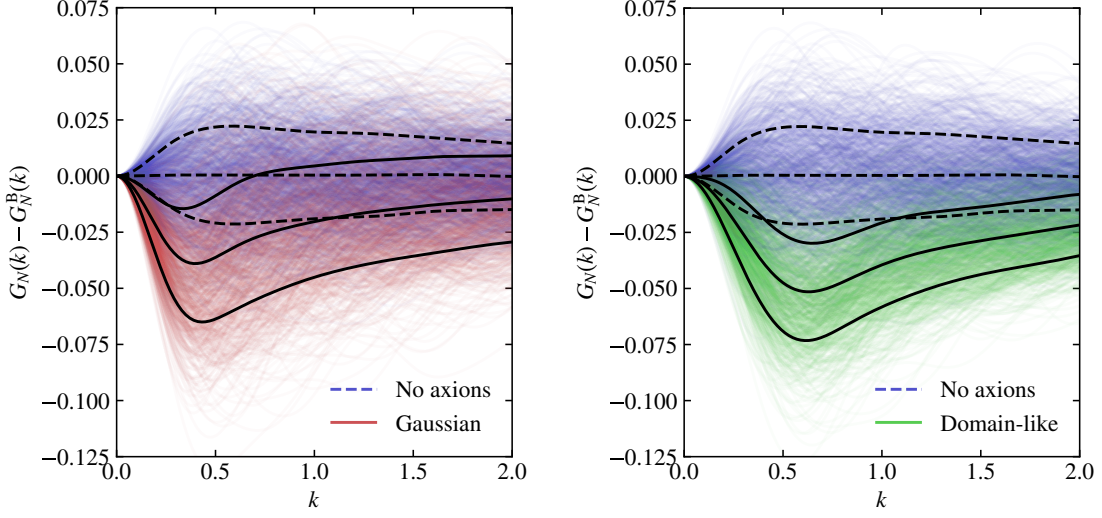
5.2 ALP wiggles

The ALP wiggles present outside the strong mixing regime (see Fig. 2) will lead to characteristic wiggles in the photon spectra. In order to extract the information about the wiggles, we can compute the discrete power spectrum

$$G_N(k) = \left| \frac{1}{N} \sum_{\text{events}} \mathrm{e}^{\mathrm{i}\eta k} \right|^2 , \tag{4}$$

where the sum goes over the detected photons. The energy parameter $\eta = \eta(E)$ has to be chosen such that it resembles the energy dependence of the wiggles. From the solution in a homogeneous magnetic field (Fig. 2), we know that one should choose $\eta \sim E^{-1}$ at small energies and $\eta \sim E$ at large energies. Here, we consider the high energy case and choose $\eta = E/E_{\min}$ with $E_{\min} = 10^{12}$ eV. This choice is an ideal application for ELMAG since one can take into account the cascade photons and energy losses on an event-by-event basis.

In Fig. 5 we plot the discrete power spectrum with the background extracted, $G_N(k) - G_N^{\mathrm{B}}(k)$, for 1000 simulated realisations of the magnetic field, both Gaussian (left; in red) and domain-like (green; right) turbulent fields. The average and its $\pm 1\sigma$ contours are shown as solid black lines. For comparison, we also show similar results obtained when ALPs are not present (blue). It is clear that there is a signal in the power spectrum due to the ALP wiggles around $k_{\text{signal}} = 0.5$.

---

[4]The energy at which this effect occur depend on the magnetic field environment. For extragalactic magnetic fields, the effect occurs in the energy window of CTA.

Figure 5: The power spectrum obtained for 1000 realisations of the magnetic field is plotted for a Gaussian turbulent field (left; in red) and domain-like field (right; in green). In order to highlight the potential signals from photon-ALP oscillations, the average power spectrum without any ALPs is extracted. The average and its $\pm 1\sigma$ variation is shown to highlight the trends in the plot. For comparison, the results for the simulations without any ALPs is shown in blue and dashed lines.

In order to quantify the strength of using the discrete power spectrum, we perform now a simple statistical test. We define the test statistics
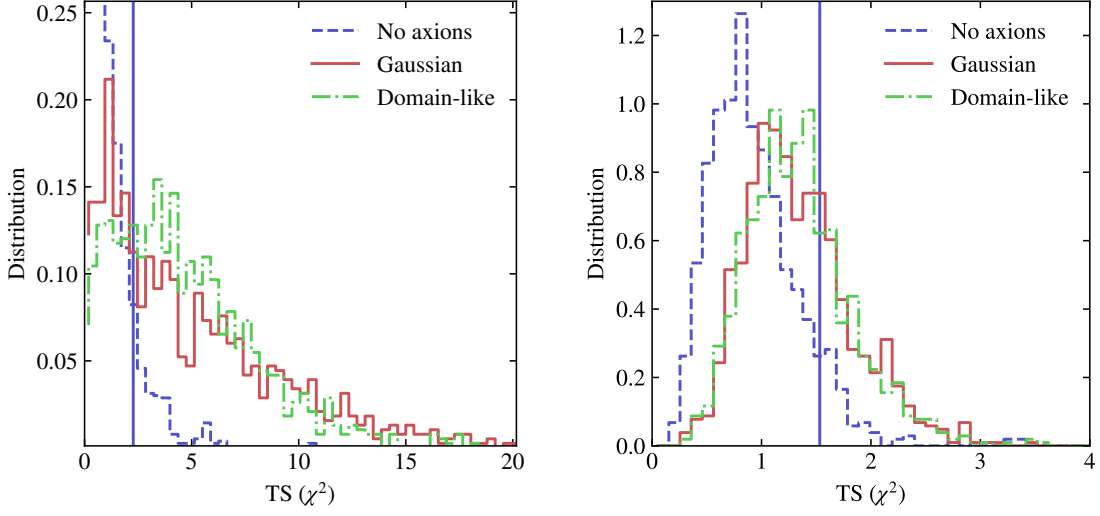
$$\text{TS} = \frac{1}{\Delta k} \int_0^{\Delta k} \frac{[G_N(k) - G_N^B]^2}{\sigma_N^B(k)^2} \, \mathrm{d}k \,, \tag{5}$$

and choose $\Delta k = 2k_{\text{signal}}$. Note that the optimal choice of Δk depends on the magnetic field properties and that the signal will depend on the choice of the energy window. For comparison, we also consider a test statistic based on the more traditional method of searching for irregularities in the photon spectrum:

$$\text{TS}_{\text{res}} = \frac{1}{N_{\text{bins}}} \sum_{\text{bins}} \frac{[\Phi(E) - \Phi^B(E)]^2}{\sigma(E)^2}, \tag{6}$$

where Φ, Φ^B and σ refer to respectively the binned spectrum, its uncertainty and the expected spectrum without ALPs in Fig. 4. The final results of the test statistics is shown in Fig. 6. Note that both test statistics we use here have the simple interpretation as the χ^2-value of a fit to the null-hypothesis. While TS_{res} will be centered around the expected value of 1, this is not necessarily true for TS due to significance inflation. Even so, it is clear that TS performs much better than TS_{res}. As a final note, neither TS nor TS_{res} have been optimised for the particular source. For example, the bin sizes can be adjusted to increase the efficiency of TS_{res}, while Δk, $E_{\min}$ and $E_{\max}$ can be adjusted to improve TS.

In order to be more concrete, we define C_{90} as the probability that a signal from a random magnetic field configuration is detected with more than 90 % confidence. In the plots, this number is the same as the area under the curves to the right hand side of the blue vertical line. Using

Figure 6: Comparison of the test statistics obtained using 1000 realisations of the considered magnetic fields. The left plot shows the distribution of TS [Eq. (5)], and the right plot TS_{res} [Eq. (6)]. The blue dashed line is the results obtained without any photon-ALP oscillations and represents thus the null-hypothesis of ALP searches. The vertical blue line represents 90 % value of the CDF of the null-hypothesis.

the power spectrum-method, we obtain $C_{90} = 0.66$ for the Gaussian turbulent field and $C_{90} = 0.75$ domain-like field. This difference is due to the larger cosmic variance in the magnetic field for the Gaussian turbulent field: the wiggles obtained for a domain-like magnetic field will be more or less at the same location due to the small variation in the transverse magnetic field. One should thus refrain from using a domain-like magnetic field in precision studies. Meanwhile, we obtain $C_{90} = 0.35$ and $C_{90} = 0.33$ with the residual method.

In addition to perform better than the test statistic TS_{res}, TS uses the energy dependence of the ALP wiggles as observable. This means that a detection using this method will lead to a less ambigous detection of photon-ALP oscillations, which further can be tested by looking at the mixing transition at lower energies. In addition, by "tuning" Δk and E_{min} after a confirmed detection of ALPs, one can infer information about the magnetic field. The test statistics can in principle further be improved by taking into account the location and shape of the signal; it may thus be an ideal task for machine learning.

6. Conclusion

The implementation of axion-like particles (ALP)s into ELMAG complements existing codes and (semi-)analytical approaches. For the first time, photon-ALP oscillations are studied in a complete Monte Carlo framework which takes into account cascade photons and absorbtion on an event-by-event basis.

By using the new code as a framework, we discussed the importance of a proper treatment of the magnetic fields: although simple magnetic field models, such as the domain-like turbulence, may reproduce similar properties as more physical models, they fail to properly reproduce e.g. the

cosmic variance. As a consequence, results relying on domain-like turbulent fields should be treated with care. Furthermore, we introduced a new statistical test that can be used to search for ALP wiggles. The approach is based on computing the discrete power spectrum of the detected photons, and it performs better than existing statistical tests on the binned energy spectrum. With the new statistical test and the upcoming Cherenkov Telescope Array (CTA), one may hope to finally use gamma-ray and X-ray observations to put limits on axionic dark matter.

References

[1] R. D. Peccei and H. R. Quinn, *CP Conservation in the Presence of Instantons*, *Phys. Rev. Lett.* **38** (1977) 1440.

[2] R. D. Peccei and H. R. Quinn, *Constraints Imposed by CP Conservation in the Presence of Instantons*, *Phys. Rev. D* **16** (1977) 1791.

[3] S. Weinberg, *A New Light Boson?*, *Phys. Rev. Lett.* **40** (1978) 223.

[4] F. Wilczek, *Problem of Strong P and T Invariance in the Presence of Instantons*, *Phys. Rev. Lett.* **40** (1978) 279.

[5] J. Preskill, M. B. Wise and F. Wilczek, *Cosmology of the Invisible Axion*, *Phys. Lett. B* **120** (1983) 127.

[6] L. F. Abbott and P. Sikivie, *A Cosmological Bound on the Invisible Axion*, *Phys. Lett. B* **120** (1983) 133.

[7] M. Dine and W. Fischler, *The Not So Harmless Axion*, *Phys. Lett. B* **120** (1983) 137.

[8] D. J. E. Marsh, *Axion Cosmology*, *Phys. Rept.* **643** (2016) 1 [1510.07633].

[9] A. Arvanitaki, S. Dimopoulos, S. Dubovsky, N. Kaloper and J. March-Russell, *String Axiverse*, *Phys. Rev. D* **81** (2010) 123530 [0905.4720].

[10] M. Cicoli, M. Goodsell and A. Ringwald, *The type IIB string axiverse and its low-energy phenomenology*, *JHEP* **10** (2012) 146 [1206.0819].

[11] H.E.S.S. collaboration, *Constraints on axionlike particles with H.E.S.S. from the irregularity of the PKS 2155-304 energy spectrum*, *Phys. Rev. D* **88** (2013) 102003 [1311.3148].

[12] Fermi-LAT collaboration, *Search for Spectral Irregularities due to Photon–Axionlike-Particle Oscillations with the Fermi Large Area Telescope*, *Phys. Rev. Lett.* **116** (2016) 161101 [1603.06978].

[13] C. S. Reynolds, M. C. D. Marsh, H. R. Russell, A. C. Fabian, R. Smith, F. Tombesi et al., *Astrophysical limits on very light axion-like particles from Chandra grating spectroscopy of NGC 1275*, 1907.05475.

[14] J. S. Reynés, J. H. Matthews, C. S. Reynolds, H. R. Russell, R. N. Smith and M. C. D. Marsh, *New constraints on light Axion-Like Particles using Chandra Transmission Grating Spectroscopy of the powerful cluster-hosted quasar H1821+643*, 2109.03261.

[15] A. Payez, C. Evoli, T. Fischer, M. Giannotti, A. Mirizzi and A. Ringwald, *Revisiting the SN1987A gamma-ray limit on ultralight axion-like particles*, *JCAP* **02** (2015) 006 [1410.3747].

[16] M. Xiao, K. M. Perez, M. Giannotti, O. Straniero, A. Mirizzi, B. W. Grefenstette et al., *Constraints on Axionlike Particles from a Hard X-Ray Observation of Betelgeuse*, *Phys. Rev. Lett.* **126** (2021) 031101 [2009.09059].

[17] C. Dessert, J. W. Foster and B. R. Safdi, *X-ray Searches for Axions from Super Star Clusters*, *Phys. Rev. Lett.* **125** (2020) 261102 [2008.03305].

[18] G. A. Pallathadka et al., *Reconciling hints on axion-like-particles from high-energy gamma rays with stellar bounds*, *JCAP* **11** (2021) 036 [2008.08100].

[19] P. Arias, D. Cadamuro, M. Goodsell, J. Jaeckel, J. Redondo and A. Ringwald, *WISPy Cold Dark Matter*, *JCAP* **06** (2012) 013 [1201.5902].

[20] CTA collaboration, *Sensitivity of the Cherenkov Telescope Array for probing cosmology and fundamental physics with gamma-ray propagation*, *JCAP* **02** (2021) 048 [2010.01349].

[21] M. Meyer, J. Davies and J. Kuhlmann, *gammaALPs: An open-source python package for computing photon-axion-like-particle oscillations in astrophysical environments*, *PoS* **ICRC2021** (2021) 557 [2108.02061].

[22] J. H. Matthews, C. S. Reynolds, M. C. D. Marsh, J. Sisk-Reynés and P. E. Rodman, *How do Magnetic Field Models Affect Astrophysical Limits on Light Axion-like Particles? An X-ray Case Study with NGC 1275*, 2202.08875.

[23] M. Kachelriess and J. Tjemsland, *On the origin and the detection of characteristic axion wiggles in photon spectra*, *JCAP* **01** (2022) 025 [2111.08303].

[24] M. Kachelriess, S. Ostapchenko and R. Tomas, *ELMAG: A Monte Carlo simulation of electromagnetic cascades on the extragalactic background light and in magnetic fields*, *Comput. Phys. Commun.* **183** (2012) 1036 [1106.5508].

[25] M. Blytt, M. Kachelriess and S. Ostapchenko, *ELMAG 3.01: A three-dimensional Monte Carlo simulation of electromagnetic cascades on the extragalactic background light and in magnetic fields*, *Comput. Phys. Commun.* **252** (2020) 107163 [1909.09210].

[26] R. A. Batista and A. Saveliev, *The Gamma-Ray Window to Intergalactic Magnetism*, 2105.12020.

[27] G. Raffelt and L. Stodolsky, *Mixing of the Photon with Low Mass Particles*, *Phys. Rev. D* **37** (1988) 1237.

[28] G. Galanti and M. Roncadelli, *Behavior of axionlike particles in smoothed out domainlike magnetic fields*, *Phys. Rev. D* **98** (2018) 043018 [1804.09443].

[29] M. Meyer, D. Montanino and J. Conrad, *On detecting oscillations of gamma rays into axion-like particles in turbulent and coherent magnetic fields*, *JCAP* **09** (2014) 003 [1406.5972].

[30] M. C. D. Marsh, J. H. Matthews, C. Reynolds and P. Carenza, *Fourier formalism for relativistic axion-photon conversion with astrophysical applications*, *Phys. Rev. D* **105** (2022) 016013 [2107.08040].

[31] Y. Grossman, S. Roy and J. Zupan, *Effects of initial axion production and photon axion oscillation on type Ia supernova dimming*, *Phys. Lett. B* **543** (2002) 23 [hep-ph/0204216].

[32] D. Wouters and P. Brun, *Irregularity in gamma ray source spectra as a signature of axionlike particles*, *Phys. Rev. D* **86** (2012) 043005 [1205.6428].

[33] A. De Angelis, G. Galanti and M. Roncadelli, *Relevance of axion-like particles for very-high-energy astrophysics*, *Phys. Rev. D* **84** (2011) 105030 [1106.1132].

[34] G. Galanti and M. Roncadelli, *Extragalactic photon–axion-like particle oscillations up to 1000 TeV*, *JHEAp* **20** (2018) 1 [1805.12055].

[35] G. Galanti, F. Tavecchio, M. Roncadelli and C. Evoli, *Blazar VHE spectral alterations induced by photon–ALP oscillations*, *Mon. Not. Roy. Astron. Soc.* **487** (2019) 123 [1811.03548].

[36] R. Buehler, G. Gallardo, G. Maier, A. Domínguez, M. López and M. Meyer, *Search for the imprint of axion-like particles in the highest-energy photons of hard γ-ray blazars*, *JCAP* **09** (2020) 027 [2004.09396].

[37] CTA Consortium collaboration, *Monte Carlo design studies for the Cherenkov Telescope Array*, *Astropart. Phys.* **43** (2013) 171 [1210.3503].

[38] A. De Angelis, M. Roncadelli and O. Mansutti, *Evidence for a new light spin-zero boson from cosmological gamma-ray propagation?*, *Phys. Rev. D* **76** (2007) 121301 [0707.4312].

[39] D. Horns and M. Meyer, *Indications for a pair-production anomaly from the propagation of VHE gamma-rays*, *JCAP* **02** (2012) 033 [1201.4711].